Condensation heat transfer in smooth inclined tubes for R134a at different saturation temperatures

Josua P. Meyer [*], Jaco Dirker[**], Adekunle O. Adelaja[***]

Department of Mechanical and Aeronautical Engineering, University of Pretoria, Private Bag X20, Hatfield 0028, Pretoria, South Africa.

**Corresponding author:*

Email: josua.meyer@up.ac.za

Phone: +27 12 420 3104,

***Alternative Corresponding Author:*

Email: jaco.dirker@up.ac.za

Phone: +27 12 420 2465

****Alternative Corresponding Author:*

Email: kunle.adelaja@up.ac.za

Abstract

This paper presents the effects of saturation temperature and inclination angle on convective heat transfer during condensation of R134a in an inclined smooth tube of inner diameter of 8.38 mm. Experiments were conducted for inclination angles ranging from -90° (vertical downwards) to +90° (vertical upwards) for mass fluxes between 100 kg/m^{2}s and 400 kg/m^{2}s and mean vapour qualities between 0.1 and 0.9 for saturation temperatures ranging between 30°C and 50°C in a test matrix of 637 test data points. The results show that saturation temperature and inclination

angle strongly influenced the heat transfer coefficient. With respect to saturation temperature, an increase in saturation temperature generally led to a decrease in heat transfer coefficient irrespective of the inclination angle. The effect of inclination angle was found to be more pronounced at mass fluxes of 100 kg/m^{2}s and 200 kg/m^{2}s for the range of mean vapour qualities considered. Within the region of influence of inclination, there was an optimum angle, which was between -15°and -30° (downward flow). The inclination effect corresponded to the predominance of the effect of gravity on the flow distribution. An increase in saturation temperature increased the effect of inclination on two-phase heat transfer.

Keywords: Experiment, condensation, heat transfer coefficient, saturation temperature, inclined tube, inclination angle

Nomenclature

A	area
c_p	specific heat
d	diameter
EB	energy balance
g	gravitational acceleration
G	mass flux
h	enthalpy
k	thermal conductivity
L	length of test section

$\dot{m}$	mass flow rate
Q	heat transfer rate
R	thermal resistance
T	temperature
x	vapour quality
z	axial direction

Greek symbols

α	heat transfer coefficient
β	inclination angle

Subscripts

Cu	copper
H_2O	water
i	inner
in	inlet
j	measurement location
l	liquid
m	mean/ average
o	outer
out	outlet
pre	pre-condenser
ref	refrigerant

sat saturation

test test condenser

v vapour

w wall

1. Introduction

Heat exchangers in heat pumps, refrigeration and air-conditioning systems play a vital role in industrial and domestic applications whether for human comfort, preservation of farm produce, or for cooling of heat-emitting appliances or equipment. These heat-exchanging systems condense at different design temperatures, for example, hot water heat pumps operate at condensing temperatures of between 50°C to 70°C, industrial chiller systems that are water-cooled condense at about 40°C, fossil fuel power stations condense at approximately 30°C to 40°C and water-source and ground-source heat pumps can condense at temperatures of 20°C – 30°C. Various researchers [1 – 2] have investigated the performance of heat exchangers at these temperatures using tubes of different sizes, orientations and tube surfaces whether smooth or inner/externally grooved such as microfins, corrugated and wire inserts.

Of particular interest in this study is the use of inclined smooth tubes subjected to different saturation temperatures as some condenser tubes in industrial application such as A-frames of dry cooling towers are not orientated horizontally but at an angle to reduce space. The only review on inclined tubes was done by Lips and Meyer [3]. The review showed that limited studies have

been conducted on convective condensation in inclined smooth tubes for the whole range of inclination angles. A brief overview is given here.

Studies on condensation heat transfer in inclined tubes for reflux condensation are considered first. Reflux condensation is increasingly applied to compact heat exchangers which are controlled by gravity. For this system, vapour enters the inclined or vertical condenser and flow upwards while the condensate flow downwards counter current under the influence of gravity. Fiedler and Auracher [4] investigated the heat transfer, flooding point and film thickness during the reflux condensation of R134a in an inclined smooth tube of 7.0 mm both theoretically and experimentally. The inclination angle was found to have significant effects on the heat transfer and flooding point. The optimum angle where the highest flooding took place was between +45° (upward flow) and +60° (upward flow) whereas the highest heat transfer occurred at close to +40° (upward flow). In the experimental study, heat transfer was investigated [5] during reflux condensation of the binary zeotropic mixture of R134a/R123 in a narrow tube (7.0 mm inner diameter and 0.5 m length) and a rectangular channel (7.0 mm hydraulic diameter and 0.5 m length). Results show that the overall heat transfer coefficient is smaller during condensation of R134a. At Reynolds numbers between 50 and 80, an enhanced heat transfer of about 20% compared with +90° inclination was observed when the inclination angle was +45°. The authors did not categorically state that +45° is the optimum inclination angle, however, they acknowledged that at Reynolds numbers higher than 80 there was no noticeable effect of inclination and also that the thinning effect of the fluid thickness at inclined position was responsible for the higher coefficient of heat transfer.

On convective condensation heat transfer, Nitheanandan and Soliman [6] investigated the effect of 10° upward and downward inclinations within the different transition lines on flow regime boundaries of condensing steam. The mass flux used was between 20 kg/m^{2}s and 280 kg/m^{2}s with a 13.8 mm inner diameter tube. Their study showed that the effect of annular flow appears to be insignificant at small inclination angles. Wang and Du [7] approached their study of film-wise condensation in small/mini diameter tubes both theoretically and experimentally. In their experiment, steam was used as the working fluid and the mass flux ranged between 10 kg/m^{2}s and 100 kg/m^{2}s for copper pipes of inner diameter of 1.94 mm, 2.8 mm, 3.95 mm and 4.98 mm. They concluded that gravity, unlike in larger tubes, had a decreasing effect on flow condensation in small/mini tubes and that the inclination effect was accountable for stratifying the fluid and thinning the liquid film. No optimum inclination angle was reported.

Wurfel *et al.* [8] examined flow condensation of n-heptane/air, water/air, and condensing n-heptane inside an inclined tube and reported that the heat transfer coefficient increased with inclination, thus the consideration of the tube inclination proved to be useful for the description of the heat transfer during film condensation in turbulent two-phase flow.

Akhavan-Behabadi *et al.* [9-11] investigated both corrugated and microfin tubes in the condensation heat transfer of R134a for low mass fluxes for the whole range of inclination angle. For microfin tubes, the mass fluxes ranged between 53 kg/m^{2}s and 212 kg/m^{2}s, vapour qualities between 0.2 and 0.8, average saturation temperature of 35°C for a tube of inner diameter of 8.92 mm. For the corrugated tube, the mass flux range was between 87 kg/m^{2}s and 253 kg/m^{2}s,

for average condensing temperatures of between 24°C and 38°C for a copper tube of inner diameter of 8.32 mm. Apart from the fact that the microfin and corrugated tubes had enhanced heat transfer, an optimum inclination angle of $+30^{o}$ (upward flow) was obtained.

Theoretical investigations of the heat transfer coefficient in R134a, R141b and R11 were carried out by Saffari and Naziri [12]. The governing differential equations of kinematics, dynamics and thermal aspects of two-phase flow were derived from a thin film flow model and solved simultaneously while numerical solutions were obtained. It was reported that the optimum angle was achieved between -30° and -50° (downward flow). For R134a, the optimum angle was -30° at saturation temperature of 30°C, for Re = 40,000. In their study, Lyulin *et al.* [13] used pure ethanol vapour in downward flow at saturation temperature of 58°C and concluded that the heat transfer coefficient reduced with an increase of temperature difference between saturation and wall temperatures. The optimum inclination angle obtained was between -15° and -35° (downward flow).

Lips and Meyer [14-16], in their study of convective condensation of R134a in a smooth tube of inner diameter of 8.38 mm, mean vapour qualities of 0.1 – 0.9, mass flux of 200 – 400 kg/m^2s for the whole range of inclination angles at saturation temperature of 40°C, reported a significant influence of inclination angle on heat transfer especially at low mass fluxes and low mean vapour qualities. In their study, optimum inclination angles of -15° and -30° (downward flow) were obtained.

More recently, Caruso *et al.* [17-18] investigated film condensation of steam in the presence of non-condensable gases in different sized tubes at different inclination angles, gas

concentrations and flow rates. It was found that the non-condensable gas concentration and flow rates had a significant influence on the heat transfer coefficient, but that the inclination effect could not be quantified fully. In another recent study, Del Col et al. [19] considered the condensation of R134a in a square minichannel at a saturation temperature of 40°C for different mass flux values and channel orientations (vertical upwards, horizontal and vertical downwards). They found that the heat transfer coefficient was only influenced by the channel orientation at low mass fluxes in the region of 100 – 135 kg/m^{2}s.

In summary, the most comprehensive work of convective condensation in inclined tubes was done by Lips and Meyer [14-16]. At different inclination angles they reported experimental measurements of heat transfer coefficients, pressure drop, mean vapour qualities, mass fluxes, and photos of the flow regimes. However, this body of work was limited to a condensation temperature of 40°C. Therefore, the purpose of this study is to expand on this work by investigating the influence of different condensing temperatures.

2. Experimental Apparatus and Test Conditions

2.1. Experimental Set-up

The experimental rig used for the study was the same test facility on which some previous experiments were conducted [14 – 16, 20, 21]. In these works, comprehensive descriptions and explanations were made. However, an overview is presented in this paper.

The test rig consisted of a vapour-compression cycle and a water cycle (Figure 1). The vapour-compression cycle consisted of two high-pressure lines (the test line and the bypass line) and a low-pressure line through which refrigerant R134a was pumped with the aid of a hermetically

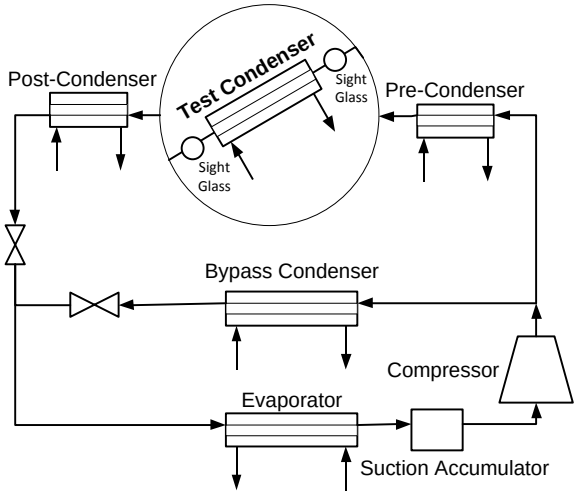

Figure 1 Schematic diagram of experimental set-up.

sealed scroll compressor with a nominal cooling load of 10 kW. Refrigerant flow in each of the high-pressure lines was controlled by electronic expansion valves (EEVs).

The test line consisted of three large condensers; the pre-condenser, test condenser and the post-condenser. The pre-condenser was used to regulate the inlet vapour quality into the test condenser where test measurements were carried out whereas the post-condenser was adjusted such that it ensured that there was complete condensation and subcooling, i.e. liquid refrigerant reached the EEV. The subcooling at the outlet of the post condenser is between 12.74°C and 34.74°C. The bypass condenser was used to control the mass flow rate, temperature and pressure of refrigerant flowing through the test section. The high-pressure lines, after the EEVs, united and led to the scroll compressor through the low-pressure line, which consisted of the evaporator and suction accumulator.

Cold and hot water were supplied by a 50 kW heating and 70 kW cooling dual-function heat pump located about 6 m above the test section. It was thermostatically controlled such that the cold and hot water were set at 15 °C – 25 °C and 40°C respectively. The hot and cold water were stored in two 5 000 *l* insulated water tanks before supplied to the set-up. While hot water ran through the evaporator, the cold was supplied to the condensers.

The test section was a copper tube-in-tube counterflow heat exchanger in which the refrigerant flowed in the inner tube and water in the annulus. It had a length of 1.488 m and had an inner-tube inside diameter of 8.38 mm and an outer tube inner diameter of 15.9 mm. The inner tube had a wall thickness of 0.6 $\pm$ 0.002 mm. To ensure that the flow through the test section was fully developed, a straight calming section, 50 diameters long, was situated at the entrance. At the inlet and outlet of the test section were sight glasses, which enabled flow visualisation and also served as insulators against axial heat conduction. A high-speed camera was installed at the outlet sight glass and used to record and document the flow patterns. A uniform Phlox backlight was positioned against the sight glass to enable good colour fidelity due to its evenly distributed light-emitting diode (LED) illumination. Three pressure taps were connected between the sight glass and test section at both sides. Two of the pressure taps were connected to different Gem sensor pressure transducers for the measurement of the absolute pressure at both inlet and outlet sides of the section so that the absolute pressure recording used on each side was the average of two pressures. The third set of pressure taps was connected together to an FP 2000 Sensotec differential pressure transducer. Flexible hoses were used to connect the test section so that it could be inclined at 90° upwards and downwards. These pressure hoses were made of Nitrile, reinforced with two high tensile steel wire braids and covered with synthetic rubber. The hoses,

which had inner diameters of 9.5 mm (3/8'') could withstand up to a pressure of 33 MPa and a temperature range of between -40°C and 100°C. These hoses were further insulated with polyethylene pipe insulation to reduce heat loss.

On the inner-tube outer wall were drilled four holes in seven equidistant stations such that at each station four, T-junction thermocouples were soldered at the top, bottom and both sides of the tubes. The 28 T-type thermocouples spanned the heat exchanger length. The refrigerant temperatures were taken at the inlet and outlet of each condenser. At each location, three thermocouples were installed, one each on the top, bottom and side of the tube wall.

The consistency of the readings at these sections was checked between the saturation temperature obtained with the absolute pressure transducers and the saturation temperature acquired from the thermocouples. Similar to the refrigerant, water inlet- and outlet temperatures were obtained at two stations. All the thermocouples used were calibrated against a high-precision Pt-100 resistance temperature detector to an accuracy of 0.1°C. Coriolis mass flow meters were used to measure the refrigerant and water flow rates. The refrigerant pressure was measured at the inlet of the test section by an analogue strain gauge transducer with an accuracy of $\pm$ 2 kPa for low mass fluxes (100 kg/m^{2}s –200 kg/m^{2}s) and ±12 kPa for high mass fluxes (G > 300 kg/m^{2}s). The measured value when used with the condensation curve provided by REFPROP [22] gave the saturation temperature, which was verified by direct measurement. The difference in the two values was found to be less than 0.1°C at high mass fluxes (400 kg/m^{2}s and above) while a higher fluctuation was observed at low mass fluxes. This, however, might be due to the non-uniformity of the flow particularly at the smooth-stratified, stratified-wavy and intermittent regions. The pressure drop across the test section was measured by a differential pressure

transducer, which was calibrated to an accuracy of $\pm$0.05 kPa. In order to determine the heat transfer rates in the pre- and post-condensers (which were needed for data processing), the water inlet and outlet temperatures as well as the water mass flow rates in these heat exchangers were also measured.

2.2. Data Acquisition and Experimental Procedure

Data from the thermocouples, pressure transducers, and Coriolis flow meters were gathered by a computerised data acquisition (DAQ) system. The DAQ system consisted of a desktop computer on which was installed a LabVIEW program written to automatically acquire needed data, an analogue/digital interface card, shielded cable assembly, signal-conditioning extensions for instrumentation (SCXI), transducer multiplexers, terminal blocks, channel multiplexers and termination units. The program displayed all measurements, including both primary and secondary quantities, which were monitored until steady state was reached before data was captured. After steady state was reached, the different sensor signals were recorded continuously through the DAQ system for about a period of 5 minutes (201 points). In order to avoid noise measurement, the average of the points was used for the calculations of the fluid properties, heat transfer coefficient and other parameters of interest.

2.3. Test conditions and methods

The test conditions described in Table 1 give the range of experimental variables used in this study and their band. Tests were conducted for the full range of inclination angles for each saturation temperature, mass flux and mean vapour quality combination as indicated in Table 2. In most cases, tests were conducted for various mass fluxes (100 – 400 kg/m^{2}s), for different

Table 1: Experimental parameters

Parameter	Range	Band
T_{sat} [°C]	30 – 50	± 0.6
G [kg/m^{2}s]	100 – 400	± 5
x_m	0.1 – 0.9	± 0.01
β [°]	-90° – +90°	± 0.1
Q_{H2O} [W]	250	± 20
Parameter	Range	Uncertainty
α [W/m^{2}K]	986 - 4291	4% – 9%

Table 2: An overview of the experimental test matrix

G [kg/m^{2}s]	T_{sat} [°C]	x_m
100	30	0.5†
	40	0.25*; 0.5*; 0.62; 0.75*
200	30	0.25*; 0.5*; 0.62; 0.75*
	35	0.25*; 0.5*
	40	0.1†; 0.25*; 0.5*; 0.62†; 0.75*; 0.9†
	45	0.1; 0.25*; 0.5*
	50	0.1†; 0.25*; 0.5*; 0.62†; 0.75*
300	30	0.5*
	35	0.5*
	40	0.1†; 0.25*; 0.5*; 0.62†; 0.75*; 0.9†
	45	0.25; 0.5*
	50	0.1†; 0.25†; 0.5*; 0.62†; 0.75†; 0.9†
400	35	0.5†
	40	0.5*; 0.62; 0.75*; 0.9
	45	0.5†
	50	0.5†; 0.75
Range of inclination angles (β) covered experimentally for each case: 0^{o}; ±5^{o}; ±10^{o}; ±15^{o}; ±30^{o}; ±60^{o}; ±90^{o}		
* = Full range of inclination angle results included † = Partial range of inclination angle results included		

mean vapour qualities (0.1 – 0.9). During the experiments, the test section water-side heat transfer was maintained between 230 W and 270 W. On the water side, the uncertainties in the heat transfer coefficient came from the uncertainties in the water temperature. On the refrigerant side, however, the uncertainties were due to the uncertainties in the saturation temperature and the wall temperature. The uncertainties in the mean inlet and outlet temperature measurement were approximately 0.1 K on both the water and refrigerant sides. However, the uncertainty in

the heat transfer coefficient was found to be between 4% and 9%. The uncertainty here refers to both the instrument (bias) uncertainties and precision uncertainties resulting from the deviation in the dataset containing 201 data points.

3. Data Reduction

Once the temperature, pressure and mass flows of the system reached steady state and the energy balance of the test condenser was stable within 3%, data was acquired. Eq. (1) was used to calculate the energy balance of the pre-, test and post-condensers.

$$EB = \frac{\left|Q_{ref} - Q_{H_2O}\right|}{Q_{ref}} \tag{1}$$

Temperature and pressure measurements were used to determine the properties of the refrigerants at the entrance of the pre-condenser and at the exit of the post-condenser. The thermophysical properties of the condensing fluid were obtained by employing data from a refrigerant property database [22].

The inlet quality, x_{in}, at the test condenser was calculated from the enthalpy of the refrigerant at the inlet, $h_{test,in}$, of the test section and the enthalpies of the liquid, h_f , and vapour, h_g, at the same condition of temperature and pressure as:

$$x_{in} = \frac{h_{test,in} - h_f}{h_g - h_f} \tag{2}$$

The enthalpy of the refrigerant at the inlet of the test section, $h_{test,in}$, was calculated from the enthalpy at the inlet of the pre-condenser, $h_{pre,in}$ (obtained using the temperature and the pressure condition at the inlet of the pre-condenser), the heat transfer rate, Q_{pre} , and the refrigerant mass flow rate, $\dot{m}_{ref}$, in the pre-condenser.

$$h_{test,in} = h_{pre,in} - \frac{|Q_{pre}|}{\dot{m}_{ref}} \tag{3}$$

The heat transfer through the pre-condenser was calculated from the water mass flow rate, $\dot{m}_{H_2O,pre}$, the specific heat capacity, c_p, and the water inlet temperature, $T_{pre,in}$, and water outlet temperature, $T_{pre,out}$:

$$Q_{pre} = \dot{m}_{H_2O,pre} c_p \left(T_{pre,in} - T_{pre,out}\right) \tag{4}$$

The vapour quality at the exit of the test section was controlled by changing the mass flow rate of the test condenser but, ensuring that Q_{test} was between 230 W and 270 W. It (x_{out}) was calculated by replacing the enthalpy at the inlet, $h_{test,\,in,}$ by the enthalpy at the outlet, $h_{test,\,out,}$ in Eq. (2) at the refrigerant saturation temperature and pressure. The enthalpy at the outlet of the test section was calculated as follows:

$$h_{test,out} = h_{test,in} - \frac{|Q_{test}|}{\dot{m}_{ref}} \tag{5}$$

The heat flow, Q_{test}, through the test condenser was obtained by replacing the mass flow rate, specific heat capacity, and the water inlet and outlet temperatures in Eq. (4) by these same parameters at the test section conditions. The mean vapour quality of the test section was obtained from the arithmetic mean of the inlet and outlet qualities: $x_m = (x_{in} - x_{out})/2$. The vapour quality difference between the inlet and outlet of the test section can be determined from the appropriate heat transfer rate and the mass flux of the R134a. This difference ranged from a minimum of 0.068 (at G = 400 kg/m^{2}s, x_m = 0.9 and T_{sat} = 40°C) to maximum of 0.238 (at G = 100 kg/m^{2}s, x_m = 0.5 and T_{sat} = 30°C). The heat transfer coefficient, α, in the test condenser was calculated from Newton's law of cooling as follows:

$$\alpha = \left| \frac{Q_{test}}{A(\overline{T}_{w,i} - T_{sat})} \right| \tag{6}$$

where A is the inner surface area of the inner tube of the test condenser, T_{sat}, is the mean of the saturation temperature at the inlet and outlet of the section. $\overline{T}_{w,i}$, is the mean inner-wall temperature and it is related to the mean outer-wall temperature, $\overline{T}_{w,o}$, of the tube through the thermal resistance of the wall of the copper tube, R_w [K/W]:

$$\overline{T}_{w,i} = \overline{T}_{w,o} + |Q_{test} R_w| \tag{7}$$

with $R_w = \ln(d_o/d_i)/2\pi k_{Cu} L$, d_o [m] being the outer diameter of the inner tube and k_{Cu} [W/mK] being the thermal conductivity of the tube wall, made of copper.

The average outer-wall temperature was calculated using the trapezoidal numerical integration:

$$\bar{T}_{w,o} = \frac{1}{L}\sum_{j=1}^{6}\left[\left(T_{w,o}^{j} + T_{w,o}^{j+1}\right)\left(z_{j+1} - z_{j}\right)\right] \tag{8}$$

where $T_{w,o}^{j}$ is the average temperature at the j^{th} location of the seven different stations and (z_{j+1} - z_j) is the distance [m] between the measurement locations.

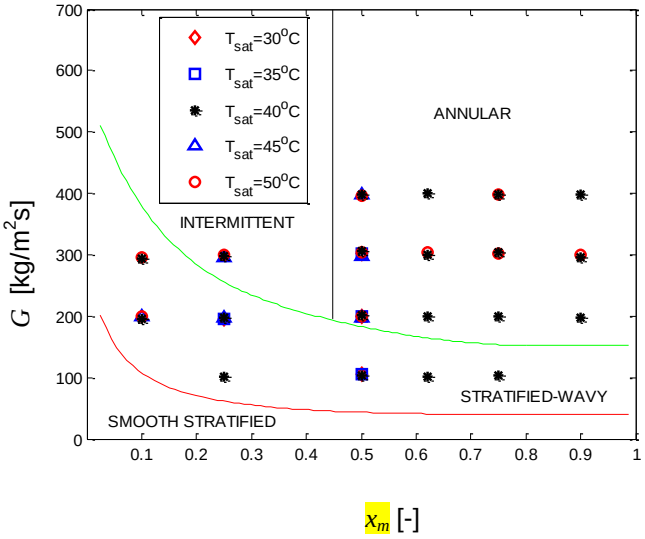

Figure 2 Experimental test points (horizontal) on the Thome-El Hajal-Cavallini [23] flow pattern map for R134a (d = 8.38 mm).

Figure 2 summarises the matrix of the experimental conditions for the horizontal orientation on the Thome-El-Hajal-Cavallini [23] flow pattern map. The conditions fell within the annular and stratified-wavy flow regimes with some test conditions also anticipated to have been in the intermittent flow regime. There are also other flow patterns observed that are not represented on this flow map based on the classification and inclination. They are, annular wavy and churn flows. The classification of flow patterns used in this study was based on Kim and Ghajar [24]. Churn flow encompasses the bubbly/slug and annular/bubbly/slug. Intermittent flow incorporates

slug, plug and elongated bubble flows [25] flow. Stratified-wavy ensues during slightly downward orientation. Liquid is mostly located at the bottom of the tube and there are waves at the liquid-vapour interface. For annular- wavy, the velocity of the vapour is increased and more liquid are at the top of the tube. Annular flow occurs as a result of high vapour velocity so that the liquid film is located uniformly or near uniformly at the perimeter of the tube. During intermittent flow, the waves at the bottom of the tube are able to reach the top. It also occurs when vapour velocity is so low that vapour is trapped in the liquid. Churn flow, which occurs mainly during or near vertical orientations (either upward or downward). It is the result of slugs of liquid collapsing into the centre of the vapour. Flooding occurred in the upward flow similar to the experience of the reflux condenser. In fact, the upward flow in this experiment typifies the reflux condenser. However, the flow pattern recorded did not take into consideration the occurrences at the base or entrance of the test section as this is not the focus of the study. The effect of flooding is captured in the churn flow that characterise the upward flow at the exit of the condenser.

The appropriate application of the flow pattern model should involve the use of the actual mass velocity and saturation temperature. However, Figure 2 was constructed using mass flux of 300 kg/m^{2}s at 40 °C saturation temperature for simplicity for all the experimental conditions. A similar test matrix was used for all other inclination angles. Table 2 gives an overview of the distribution of the 637 test data points in terms of the saturation temperature, T_{sat}, mean vapour quality, x_m, mass fluxes, G, and inclination angles, β respectively. This table also indicates which data sets are reported on fully and which data sets are reported on partially in this paper. More data points were obtained at saturation temperatures of 40^{o}C and 50^{o}C. Attention was given to

these temperatures for the reason that most water-cooled industrial heat exchange systems and hot water heat pumps operate within this range.

4. Data Comparison with other Investigations and Correlations

It was imperative to establish and test the integrity of the experimental apparatus and hence the data also. Forty-nine experimental test conditions (for horizontal flow only) of the condensation of R134a inside a smooth inclined tube were compared with six different well-established convective heat transfer correlation models. This was necessary because most of the earlier studies on heat transfer experiments and correlations were developed for this orientation.

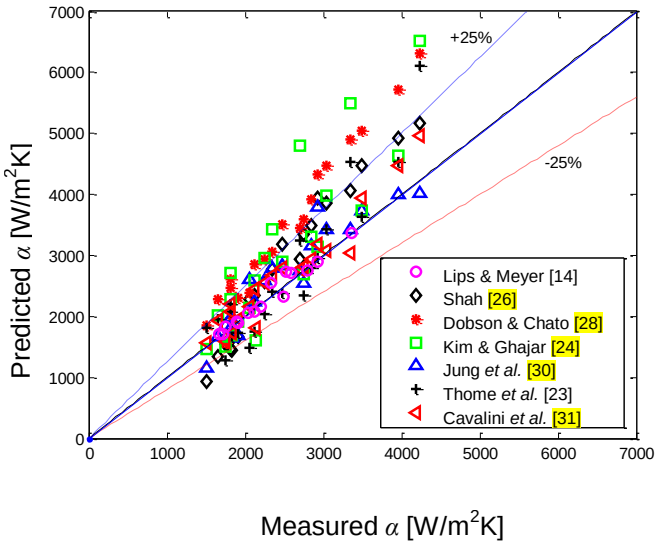

Figure 3 A comparison between experimental heat transfer results and different correlations for horizontal flow at $T_{sat} = 40^{\circ}$C.

Figure 3 displays the comparison at a saturation temperature of 40^{o}C. The correlation of Shah [26] was aimed at predicting the heat transfer coefficient irrespective of the tube orientation. It was based on a two-phase multiplier for condensation in single phase proposed by Dittus and

Boelter [27] and it is capable of predicting flow in horizontal, vertical and inclined tubes. Dobson and Chato [28] improved on Chato [29] by including a stratified-wavy model. Jung *et al.* [30] on the other hand modified the correlation of Dobson and Chato [28] and included the heat and mass flux ratio to arrive at their model. Furthermore, the model of Thome *et al.* [23] was based on the flow pattern map while the model of Cavallini *et al.* [31] was established on two different flow regimes depending on whether the heat transfer coefficient was dependent on the condensation heat flux or otherwise. Meanwhile, the heat flux is a function of the temperature difference between the saturation and tube wall temperature. Finally, the model of Kim and Ghajar [24] employed a two-phase heat transfer model developed for vertical pipe flow with modified constants to predict air-water, silicon-air, water-helium and water-Freon 12 data for horizontal orientation.

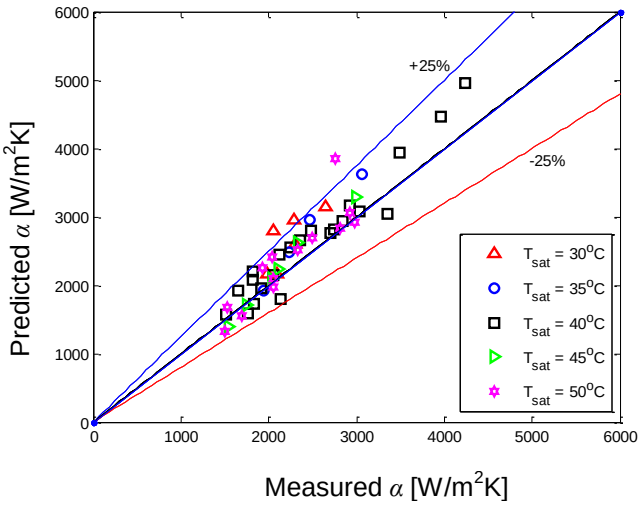

Figure 4 Comparison of experimental heat transfer data with the correlation of Cavallini *et al*. [31] for horizontal flow (β = 0°) at different saturation temperatures.

The models of Shah [26], Kim and Ghajar [24] and Jung *et al.* [30] underestimated the horizontal experimental data for low mass fluxes and low mean qualities whereas for high mass fluxes and/or high mean vapour qualities, Dobson and Chato [28], and Kim and Ghajar [24] overpredicted the data. However, the models of Thome *et al.* [23] and Cavallini *et al.* [31] are in very good agreement (within ± 25%) with horizontal tube data. Also, the current experimental data points are in good agreement (within ± 10%) with the data of Lips and Meyer [14]. For the Cavallini correlation, this is shown in Figure 4 for different saturation temperatures for the case of horizontal tube orientation. The correlation only overpredicted a few data points for T_{sat} = 30°C and 50°C (the rest were within ±20%). Based on this, it was concluded that the current experimental set-up and the associated test procedure and data sets had acceptable integrities.

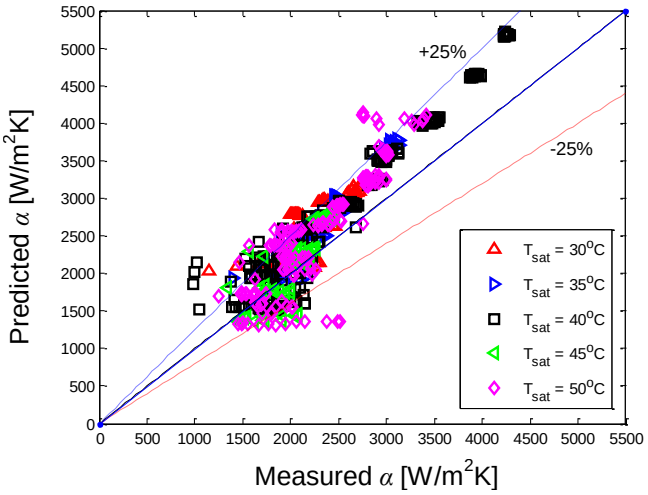

Figure 5 Comparison of experimental data for different inclinations with the correlation of Cavallini *et al.* [31] at different saturation temperatures.

Figures 5 and 6 include data points for other inclination angles. Figure 5 shows the graph of the heat transfer coefficient of the experimental data according to the saturation temperatures and inclination angles as predicted by Cavallini *et al.* [31]. The result shows that most of the data

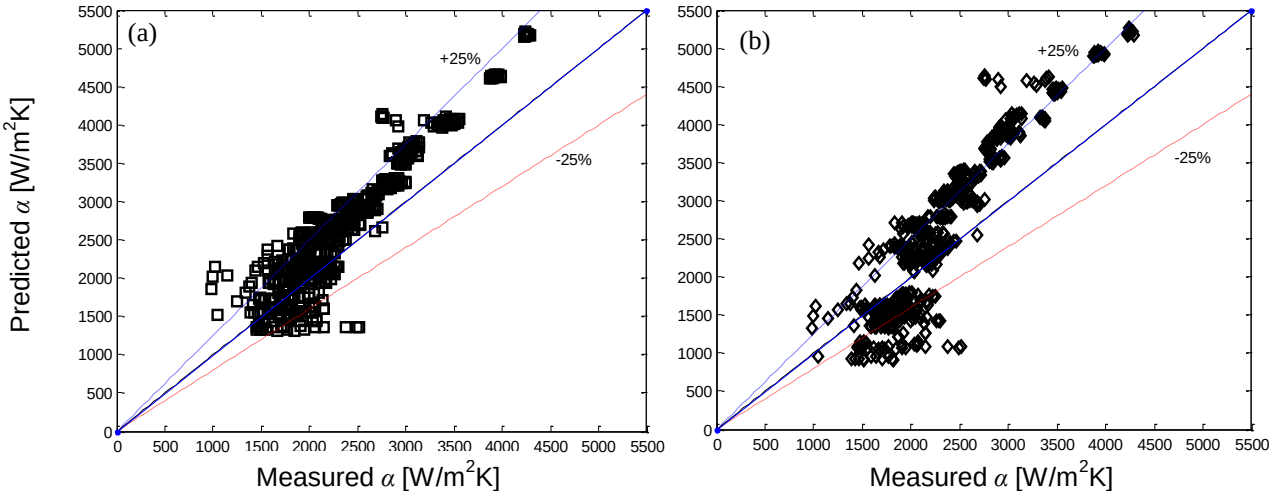

Figure 6 Comparison of experimental data at different saturation temperatures, inclination angles and mean vapour qualities with the correlation of a) Cavallini *et al.* [31] and b) Shah [26]

points irrespective of the saturation temperatures are within ± 25%. Figures 6(a) and 6(b) show the comparison of the data points for the different inclination angles with the correlations of Cavallini *et al.* [31] and Shah [26] respectively. The results indicate that more data points are within the ± 25% of the Cavallini *et al.* [31] correlation than the Shah [26]. The model of Cavallini *et al.* [31], therefore, shows a better performance in predicting the data points when compared with that of Shah [26]. In Figures 5 and 6 most of the data points that are outside the 25% error lines are for experimental points with low heat transfer coefficients.

5. Effect of Inclination, Saturation Temperature, Mean vapour quality and Mass Flux

In this section, the experimentally observed influence of the inclination angle, saturation temperature, mean vapour quality and mass flux on the heat transfer coefficients will be discussed.

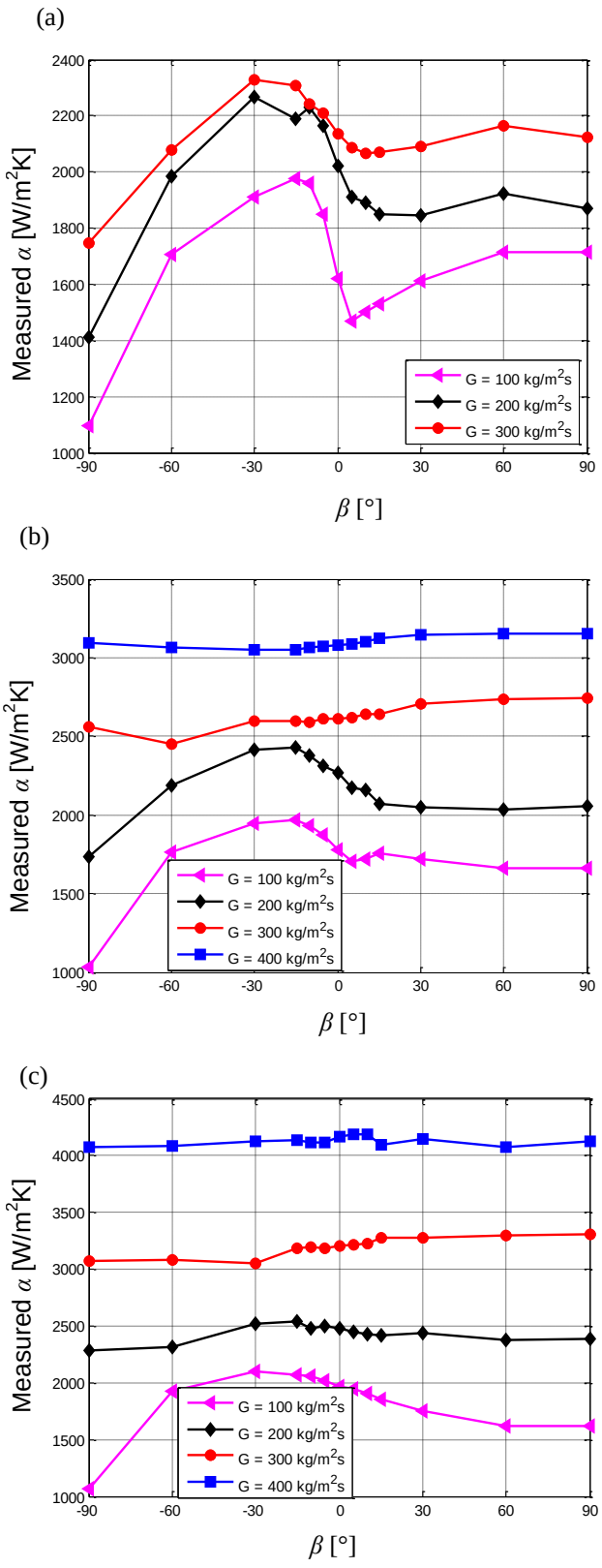

Figure 7 Inclination and mass flux effects on the heat transfer coefficient for T_{sat} = 40°C and a) x_m = 0.25, b) x_m = 0.5, c) x_m = 0.75.

Figure 7 shows the influence of the inclination angle and mass flux for mean vapour qualities of 0.25, 0.5 and 0.75 at a saturation temperature of 40 °C. The inclination angle has a significant impact on the heat transfer coefficient. The effect of inclination is pronounced between -90^{o} (vertical downwards) and +15° (slightly inclined upwards) for lower mass flux and mean vapour quality cases with the highest heat transfer coefficient occurring at inclination angles values between -30° and -15° (slightly inclined downwards). This is because of the stratifying effect of gravity, which make the liquid film at the bottom of the tube thinner. It could be noted that the thinner the liquid film is, the smaller the thermal resistance, hence the higher effective heat transfer coefficients. This agrees with the findings of Lips and Meyer [14]. The effect of inclination decreases, however, as mass flux increases, especially at mean vapour qualities of 0.5 and 0.75, until at high mass fluxes no significant observable impact of the inclination angle is present. This is because at high mass fluxes, high heat transfer coefficient was obtained during annular and annular-wavy due to the thin condensate film which are located ate the perimeter of the tube. In general, an increased mass flux resulted in increased heat transfer coefficient.

Since inclination effect is prominent at low mass flux and or low mean vapour quality, it is reasonable to consider in more detail mass flux of 300 kg/m^{2}s or less. Figure 8 shows the impact of the inclination angle and saturation temperature for mean vapour qualities of 0.25, 0.5 and 0.75 at a mass flux of 200 kg/m^{2}s, while Figure 9 does the same for a mean vapour quality of 0.5 at a mass flux of 300 kg/m^{2}s. Figure 8 shows that for mean vapour qualities of 0.25 and 0.5, irrespective of the saturation temperature, the effects of the inclination angle on the heat transfer coefficient are similar and that an optimum inclination angle of between -15° and -30^{o} (downwards flow) was obtained. In these cases, the lowest heat transfer coefficient was measured

(a)

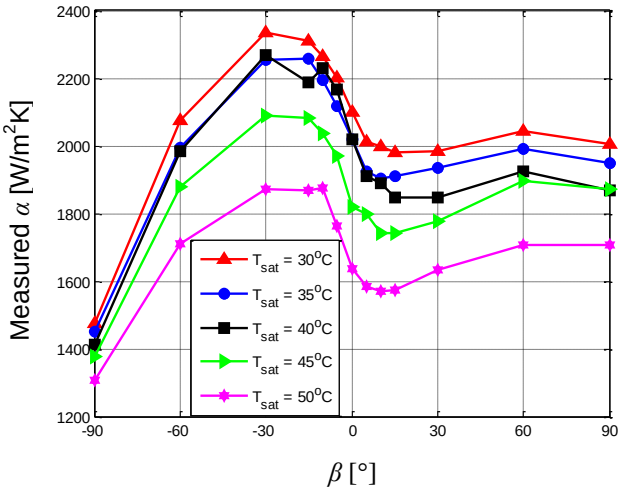

(b)

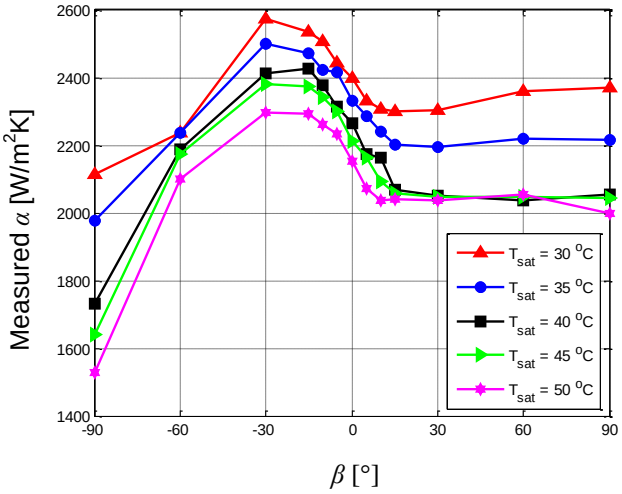

(c)

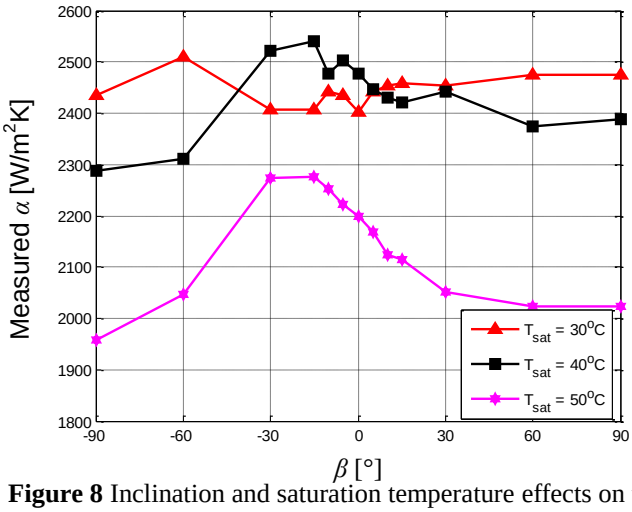

Figure 8 Inclination and saturation temperature effects on the heat transfer coefficient for G = 200 kg/m^{2}s, and a) x_m = 0.25, b) x_m = 0.5, c) x_m = 0.75.

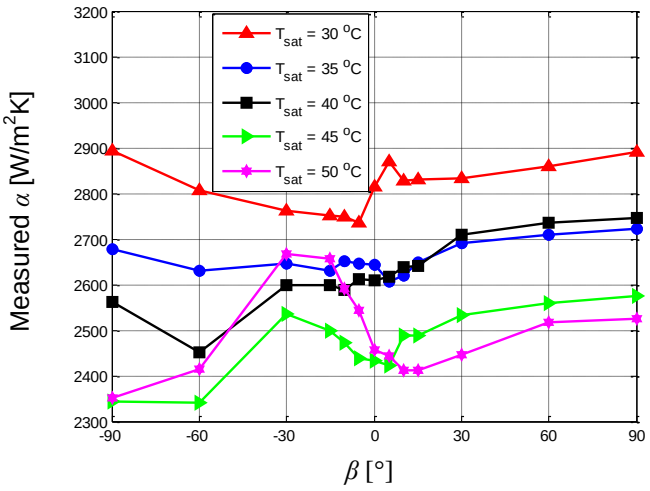

Figure 9 Inclination and saturation temperature effects on the heat transfer coefficient for G = 300 kg/m^{2}s and

for vertical downwards flow. For a mean vapour quality of 0.25, a local minimum in the heat transfer coefficient was present at inclination angles between 10° and 30° (slightly upwards flow), while for a mean vapour quality of 0.5, such a local minimum was less significant. For a higher mean vapour quality of 0.75, a similar optimum angle of between -15° and -30° was observed for saturation temperature of 40°C and 50°C, but not for 30°C, where the effect of the inclination angle was relatively weak. In general, the heat transfer coefficient increases with a decrease of saturation temperature. For example, at an inclination angle of -30°, mass flux of 200 kg/m^{2}s, and a mean vapour quality of 0.5, the heat transfer coefficient at a saturation temperature of 30^{o}C was 12% higher than for 50^{o}C.

For the case when the mass flux was 300 kg/m^{2}s and the mean vapour quality was 0.5 as shown in Figure 9, it can be seen that for a saturation temperature of 45°C and 50°C, an optimum inclination angle of -30° (downwards flow) was obtained and that a local minimum in the heat transfer coefficient was observed at inclination angles between 5° and 10° (upwards flow). The

enhancement effect was greater for 50 °C such that the heat transfer resulting from the inclination effect at 50°C supersedes the shear effect that governs the annular flow at 40°C and 35°C for inclination angles between -45° and 0°. For saturation temperatures of 30°C, 35°C and 40°C, observable patterns in the data could not be identified. In fact for a saturation temperature of 30°C, a slightly downwards inclination (-5°) exhibited the lowest heat transfer coefficients. On the effect of the saturation temperature on the heat transfer coefficient, at higher saturation temperatures, a lower heat transfer coefficient corresponds to a lower pressure drop [32]. Refrigerant properties such as density ρ , viscosity μ , thermal conductivity *k*, heat capacity c_p etc. affect the heat transfer coefficient with different degrees of sensitivity or by different extents. The most prominent of them, which decreases with increase in saturation temperature, is the liquid thermal conductivity k_l of the liquid film. That is, k_l is greater for T_{sat} = 30°C than for T_{sat} = 50°C hence, a higher heat transfer coefficient occurred at T_{sat} = 30 °C i.e. $\alpha_{30^o} > \alpha_{35^o} > \alpha_{40^o} > \alpha_{45^o} > \alpha_{50^o}$

Therefore, from the above results it can be concluded that an optimum inclination angle of between -15° and -30° exists at a combination of low mass flux, low mean vapour quality and high saturation temperature. Up to mass flux of 300 kg/m^{2}s, the saturation temperature in the test range increases the tendency of refrigerant respond to gravitational effect (i.e. to stratify). For a mean vapour quality of 0.5, at saturation temperatures below 45 °C for the case when the mass flux was 300 kg/m^{2}s and at all higher mass fluxes, annular flow predominated.

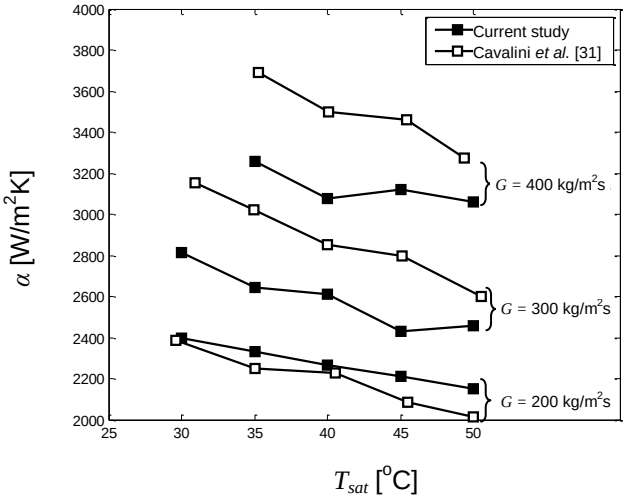

Figure 10 Comparison of the effect of saturation temperature on experimental heat transfer coefficient for different mass fluxes with Cavallini *et al*. [31] for x_m = 0.5 and β = 0°.

Figure 10 shows the dependence of the heat transfer coefficient on the saturation temperature for both the experimental data and the prediction of the Cavallini *et al*. [31] correlation for a mean vapour quality of 0.5 in a horizontal tube (β = 0°). This confirms that the heat transfer coefficient generally decreases with increasing saturation temperature for mass fluxes of 200 kg/m^{2}s, 300 kg/m^{2}s and 400 kg/m^{2}s as is evident from both the experimental and predicted trends. Considering the Cavallini *et al*. [31] correlation prediction, it was found that it overpredicted the experimental data by between 5% and 14% for mass fluxes of 300 kg/m^{2}s and 400 kg/m^{2}s. It, however, underpredicted the data points for mass fluxes of 200 kg/m^{2}s by between 0.4% and 7%.

Figure 11 shows the heat transfer coefficient in terms of mass flux and saturation temperature for inclination angles of 0° and -30°. The inclination of -30° is chosen since a large proportion of test conditions exhibited optimum heat transfer coefficients at this angle. It is evident that an

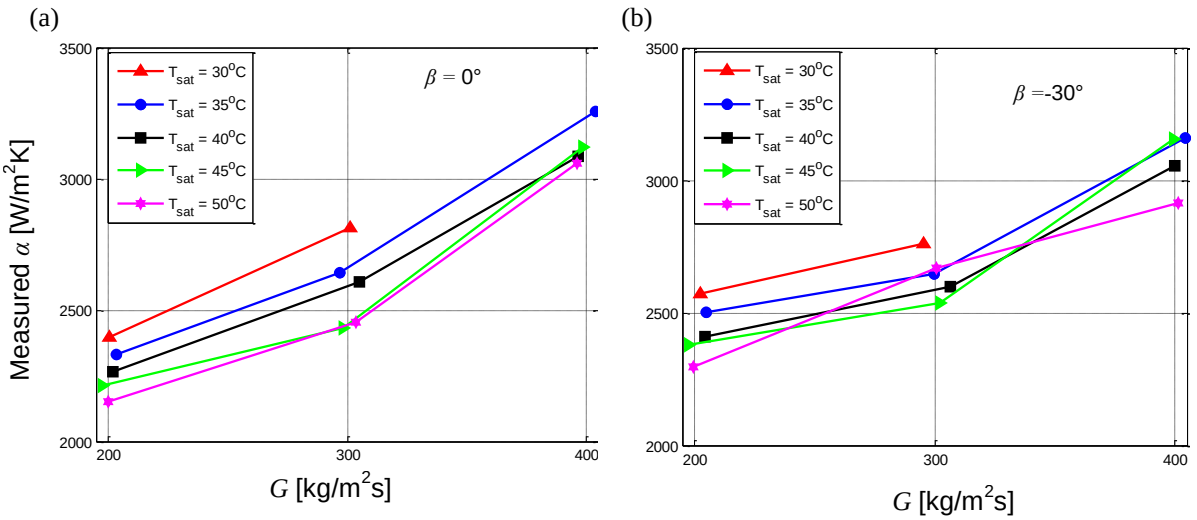

Figure 11 Effect of mass flux and saturation temperature on heat transfer coefficient for x_m = 0.5 with a) β = 0° and b) β = -30°.

increased mass flux resulted in an increased heat transfer coefficient. For all saturation temperatures the heat transfer coefficient was higher for an inclination angle of -30° (compared to 0°) for mass fluxes of 200 kg/m^{2}s and 300 kg/m^{2}s. For 400 kg/m^{2}s, where an annular flow regime is prevalent, the opposite was true. In Figure 12, the influence of the mean vapour quality is exhibited for saturation temperatures of 40°C and 50°C, at mass fluxes of 200 kg/m^{2}s and 300 kg/m^{2}s, and for various inclination cases. It can be seen that generally higher mean vapour qualities resulted in higher heat transfer coefficients.

It was also found that the heat transfer coefficient was higher for saturation temperature of 40^{o}C (compared with 50^{o}C) when the mean vapour quality is greater than 0.5 but, outside this region no specific trend was noticed, only that the maximum heat transfer coefficient was obtained at an inclination angle of -30° and the minimum at an inclination angle of -90°. It can also be seen that the effect of inclination decreases as the mean vapour quality increases. For

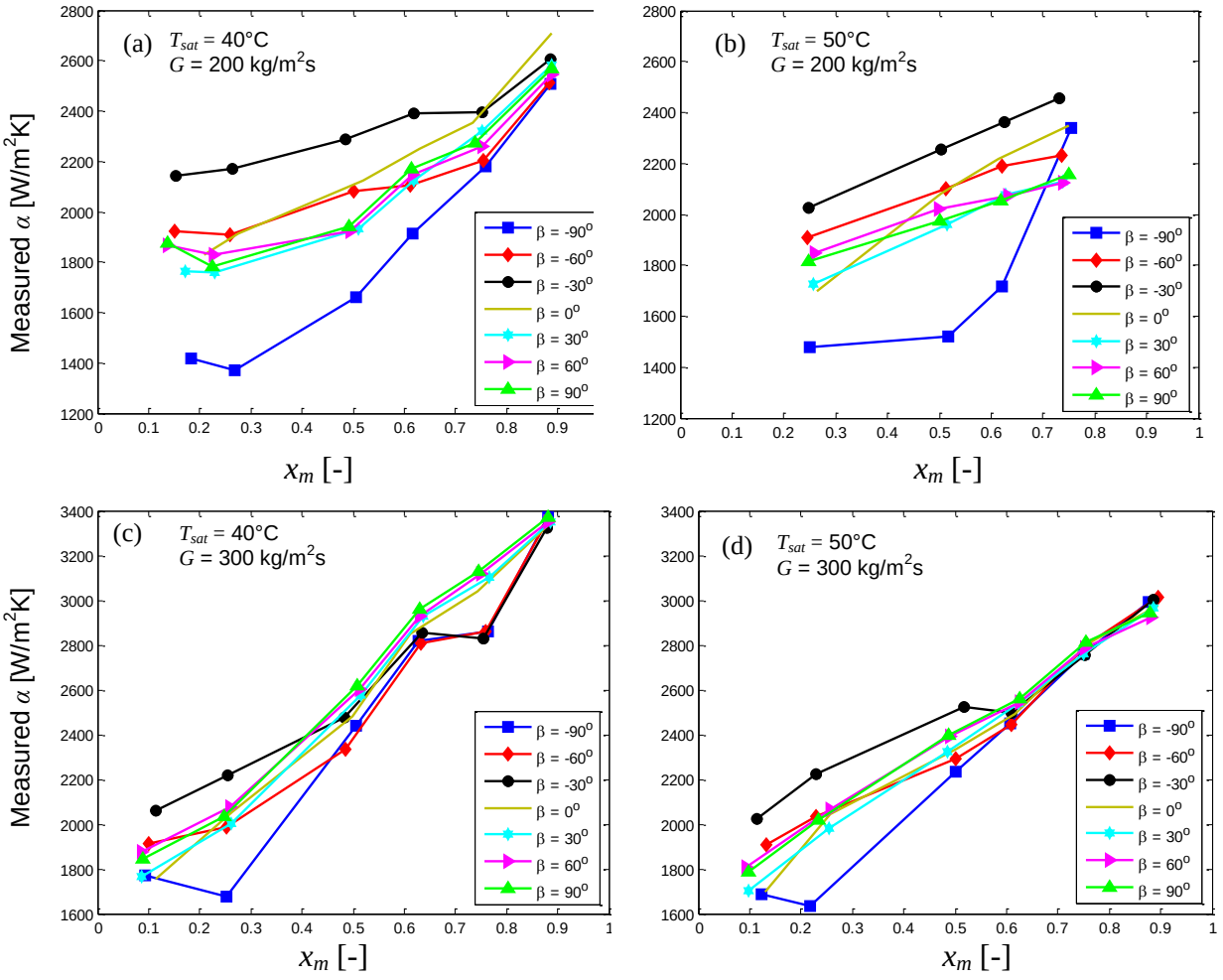

Figure 12 Comparing the effect of mean vapour qualities on heat transfer coefficient for a) G = 200 kg/m^{2}s and T_{sat} = 40°C, b) G = 200 kg/m^{2}s and T_{sat} = 50°C, c) G = 300 kg/m^{2}s and T_{sat} = 40°C, d) G = 300 kg/m^{2}s and T_{sat} = 50°C

mass fluxes of 200 kg/m^{2}s, the difference in the heat transfer coefficient between the maximum (at β = -30°) and minimum (at β = -90°) for a mean vapour quality of 0.1 was 726 W/m^{2}K (about 51% above the minimum) and for a mean vapour quality of 0.9 was 202 W/m^{2}K (about 8% above minimum) for a saturation temperature of 40^{o}C (Figure 12a). For a saturation temperature of 50^{o}C, the difference was 502 W/m^{2}K (40% above the minimum) for a mean vapour quality of

0.25 and 273 W/m^{2}K (15% above the minimum) for a mean vapour quality of 0.75 (Figure 12b). For a mass flux of 300 kg/m^{2}s, at low mean vapour qualities, the effect of the optimum inclination angle increased with the saturation temperature. For a saturation temperature of 40^{o}C, the highest heat transfer coefficient was observed at an inclination angle of -30^o when the mean vapour quality was between 0.1 and 0.4 (Figure 12c). However, for a saturation temperature of 50^{o}C, the highest heat transfer coefficient was observed for an inclination angle of -30^o at mean vapour qualities between 0.1 and 0.62 (Figure 12d). An increase in the saturation temperature somehow caused an increase in the range of mean vapour qualities where the inclination effect was dominant.

6. **Conclusions**

In this study, experiments in convective condensation were performed in a smooth inclined tube of angle varying between -90^o (vertical downwards) and +90^o (vertical upwards) using R134a as the working fluid. Experiments were conducted over a range of saturation temperature (between 30 °C and 50 °C) for mean vapour qualities of 0.1 - 0.9, mass fluxes of 100 kg/m^{2}s – 400 kg/m^{2}s while the heat transfer rate on the water side was maintained at 230 W – 270 W.

The effects of inclination angles and saturation temperature were investigated with respect to heat transfer coefficient. Generally, heat transfer coefficients increase with mass flux and mean vapour quality and the effect of inclination is more pronounced at low mass fluxes, low mean vapour qualities and high saturation temperature. At high mass fluxes (300 – 400 kg/m^{2}s), high heat transfer coefficients were obtained during annular and annular-wavy because the thin condensate film were located ate the perimeter of the tube. For low mass fluxes (100 – 200

kg/m^{2}s), high heat transfer coefficients were obtained during the slightly downward (-15^o to -30^o) because of the stratifying effect of gravity which made the liquid film at the bottom of the tube thinner. It would be noted that the thinner the liquid the smaller the thermal resistance, hence the higher heat transfer rate.

With respect to the saturation temperature, heat transfer usually reduces irrespective of the inclination angles and mass fluxes. This has been found to be because at higher saturation temperature, lower heat transfer corresponds to lower pressure drop. In addition, refrigerant properties play a major role in this regard by different degree of sensitivity or by different extent. However, prominent among these properties is the thermal conductivity of the liquid film, which decreases with temperature consequent upon which the thermal resistance increase and heat transfer coefficient decreases. Furthermore, the effect of inclination is more pronounced at higher saturation temperatures. The study clearly shows that saturation temperature has a significant influence on the heat transfer coefficient, even, on inclination effect and mass flux. Furthermore, at higher saturation temperatures especially for the case where G = 300 kg/m^{2}s, the effect of inclination can be pronounced up to x_m = 0.62. Therefore, flow pattern distribution and other flow parameters are subject to change with saturation temperature.

Acknowledgements

The funding obtained from the NRF, TESP, Stellenbosch University/ University of Pretoria, SANERI/SANEDI, CSIR, EEDSM Hub and NAC is acknowledged and duly appreciated.

References

[1] A. Cavallini, G. Censi, D. Del Col, L. Doretti, G. A. Longo, L. Rossetto, C. Zilio, Condensation inside and outside smooth and enhanced tubes - a review of recent research, Int. J. Refrigeration 26 (2003) 373-392.

[2] A. S. Dalkilic, S. Wongwise, Intensive literature review of condensation inside smooth and enhanced tubes, Int. J. Heat and Mass Transfer 52 (2009) 3409-3426.

[3] S. Lips, J. P. Meyer, Two-phase flow in inclined tubes with specific reference to condensation: a review, Int. J. Multiphase Flow 37 (2011) 845-859.

[4] S. Fiedler, H. Auracher, Experimental and theoretical investigation of reflux condensation in an inclined small diameter tube, Int. J. Heat Mass Transfer 47 (2004) 4031-4043.

[5] T. Klahm, H. Auracher, F. Ziegler, Heat transfer during reflux condensation of R134a/R123 mixture in vertical and inclined narrow tubular and rectangular channels, Int. J. Refrigeration 33 (2010) 1319-1326.

[6] T. Nitheanandan, M. H. Soliman, Influence of tube inclination on the flow region boundaries of condensing steam, Can. J. Chem. Eng. 71 (1993) 35-41.

[7] B. -X. Wang, X. -Z. Du, Study on laminar film-wise condensation for vapour in an inclined small/mini-diameter tube, Int. J. Heat Mass Transfer 43 (2000) 1859-1868.

[8] R. Wurfel, T. Kreutzer, W. Fratzscher, Turbulence transfer processes in a diabatic and condensing film flow in inclined tube, Chem. Eng. Technol. 26 (2003) 439-448.

[9] M.A. Akhavan-Behabadi, R. Kumar, S.G. Mohseni, Condensation heat transfer of R134a inside a microfin tube with different tube inclinations, Int. J. Heat Mass Transfer 50 (2007) 4864-4871.

[10] D. Khoeini, M.A. Akhavan-Behabadi, A. Saboonchi, Experimental study of condensation heat transfer of R134a flow in corrugated tubes with different inclinations, Int. Comm. Heat Mass Transfer 39 (2012) 138-143.

[11] S. G. Mohseni, M.A. Akhavan-Behabadi, Visual study of flow patterns during condensation inside a microfin tube with different inclinations, Int. Comm. Heat Mass Transfer 38 (2011) 1156-1161.

[12] H. Saffari, V. Naziri, Theoretical modelling and numerical solutions of stratified condensation in inclined tubes, J. Mech. Sci. Technol. 24 (2010) 2587-2596.

[13] Y. Lyulin, I. Marchuk, S. Chikov, O. Kabov, Experimental study of laminar convective condensation of pure vapour inside an inclined circular tube, Microgravity Sci. Technol. 23 (2011) 439-445.

[14] S. Lips, P. J. Meyer, Experimental study of convective condensation in an inclined smooth tube. Part 1: inclination effect on flow pattern and heat transfer coefficient, Int. J. Heat and Mass Transfer 55 (2012a) 395-404.

[15] S. Lips, P. J. Meyer, Experimental study of convective condensation in an inclined smooth tube. Part II: inclination effect on pressure drops and void fractions, Int. J. Heat and Mass Transfer 55 (2012b) 405-412.

[16] S. Lips, P. J. Meyer, Stratified flow model for convective condensation in an inclined tube, Int. J. Heat and Fluid Flow 36 (2012) 83-91.

[17] G. Caruso, D. Vitale Di Maio, A. Naviglio, Condensation heat transfer coefficient with noncondensable gases inside near horizontal tubes, Desalination 309 (2013) 247- 253.

[18] G. Caruso, D. Vitale Di Maio, A. Naviglio, Film condensation in inclined tubes with noncondensable gases: An experimental study on the local heat transfer coefficient, Int. Comm. Heat Mass Transfer 45 (2013) 1-10.

[19] D. Del Col, M. Bortolato, S. Bortolin, M. Azzolin, Minichannel condensation in downward, upward and horizontal configuration, J. Physics: Conference Series 395 (1) (2012), art. No. 012092.

[20] E. Van Rooyen, M. Christians, L. Liebenberg, J. P. Meyer, Probabilistic flow pattern-based heat transfer correlation for condensing intermittent flow in smooth horizontal tubes, Int. J. Heat and Mass Transfer 53 (2010) 1446-1460.

[21] R. Suliman, L. Liebenberg, J. P. Meyer, Improved flow pattern map for accurate prediction of the heat transfer coefficient during condensation of R134a in smooth horizontal tubes and within the low-mass flux range, Int. J. Heat and Mass Transfer 52 (2009) 5701-5711.

[22] REFPROP., NIST Thermodynamic properties of refrigerants and refrigerant mixtures (REFPROP), version 8.0, NIST Standard Reference Database 23, National Institute of Standards and Technology, Gaithersbury, MD, 2005.

[23] J. R. Thome, J. El Hajal, A. Cavallini, Condensation in horizontal tubes. Part II: new heat transfer model based on flow regimes, Int. J. Heat and Mass Transfer 46 (2003) 3365-3387.

[24] D. Kim, A. J. Ghajar, Heat transfer measurement and correlations for air-water flow of different flow patterns in a horizontal pipe, Exp. Thermal Fluid Sci. 25 (2002) 659-676.

[25] S.L. Kokal, J.F. Stanislav, An experimental study of two-phase in slightly inclined pipes – 1. Flow pattern, Chem. Eng. Sci. 44 (3) (1989) 665 - 679.

[26] M. Shah, A general correlation for heat transfer during film condensation inside pipes, Int. J. Heat and Mass Transfer 22 (1979) 547-556.

[27] F. W. Dittus, L. M. K. Boelter, Heat transfer for automobile radiators of the tubular type, Publications in Engineering, University of California, Berkeley 2 (1930) 443.

[28] M. Dobson, J. Chato, Condensation in smooth horizontal tubes, ASME J. Heat Transfer 120 (1998) 193-213.

[29] J. C. Chato, Laminar condensation inside horizontal and inclined tubes, Massachusetts Inst. Technol. 1960.

[30] D. Jung, K. Song, Y. Cho, S. Kim, Flow condensation heat transfer coefficients of pure refrigerant, Int. J. Refrigeration 26 (2003) 4-11.

[31] A. Cavallini, D. Del Col, L. Doretti, M. Matkovic, L. Rossetto, C. Zilio, G. Censi, Condensation in horizontal smooth tubes: a new heat transfer model for heat exchanger design, Heat Transfer Eng. 27 (2006) 31-38.

[32] A. Cavallini, G. Censi, D. DelCol, L. Doretti, L. Rosetto, Heat transfer coefficient of HFC refrigerants during condensation at high temperature inside an enhanced tube, Int. Refrigeration and Air Conditioning Conference, paper 563.